

Pathogenic lipid-binding antiphospholipid antibodies are associated with severity of COVID-19

Anne Hollerbach¹  | Nadine Müller-Calleja^{1,2} | Denise Pedrosa² | Antje Canisius¹ | Martin F. Sprinzi³  | Tanja Falter¹ | Heidi Rossmann¹  | Marc Bodenstein⁴ | Christian Werner⁴ | Ingo Sagoschen⁵ | Thomas Münzel⁵ | Oliver Schreiner³ | Visvakanth Sivanathan³ | Michael Reuter³ | Johannes Niermann³ | Peter R. Galle³ | Luc Teyton⁶ | Wolfram Ruf^{2,6}  | Karl J. Lackner¹ 

¹Institute of Clinical Chemistry and Laboratory Medicine, Johannes Gutenberg University Medical Center Mainz, Germany

²Center for Thrombosis and Hemostasis (CTH), Johannes Gutenberg University Medical Center Mainz, Mainz, Germany

³Department of Medicine I, Johannes Gutenberg University Medical Center Mainz, Mainz, Germany

⁴Department of Anesthesiology, Johannes Gutenberg University Medical Center Mainz, Mainz, Germany

⁵Department of Cardiology, Johannes Gutenberg University Medical Center Mainz, Mainz, Germany

⁶Department of Immunology and Microbiology, Scripps Research, La Jolla, California, USA

Correspondence

Karl J. Lackner, Institute of Clinical Chemistry and Laboratory Medicine, Johannes Gutenberg University Medical Center, D-55101 Mainz, Germany.
Email: karl.lackner@unimedizin-mainz.de

and

Wolfram Ruf, Center for Thrombosis and Hemostasis, Johannes Gutenberg University Medical Center, D-55101 Mainz, Germany.
Email: ruf@uni-mainz.de

Funding information

National Heart, Lung, and Blood Institute, Grant/Award Number:

Abstract

Background: Coronavirus disease 19 (COVID-19)-associated coagulopathy is a hallmark of disease severity and poor prognosis. The key manifestations of this prothrombotic syndrome—microvascular thrombosis, stroke, and venous and pulmonary clots—are also observed in severe and catastrophic antiphospholipid syndrome. Antiphospholipid antibodies (aPL) are detectable in COVID-19 patients, but their association with the clinical course of COVID-19 remains unproven.

Objectives: To analyze the presence and relevance of lipid-binding aPL in hospitalized COVID-19 patients.

Methods: Two cohorts of 53 and 121 patients from a single center hospitalized for PCR-proven severe acute respiratory syndrome–coronavirus 2 infection were analyzed for the presence of aPL and clinical severity of COVID-19.

Results: We here demonstrate that lipid-binding aPL are common in COVID-19. COVID-19 patients with lipid-binding aPL have higher median concentrations of C-reactive protein and D-dimer, and are more likely to have a critical clinical course and fatal outcome. Lipid-binding aPL isolated from COVID-19 patients target the recently described cell surface complex of lysobisphosphatidic acid (LBPA) with the protein C receptor (EPCR) to induce prothrombotic and inflammatory responses in monocytes and endothelial cells. We show that B1a cells producing lipid-reactive aPL of the IgG isotype circulate in the blood of COVID-19 patients. In vivo, COVID-19 aPL accelerate thrombus formation in an experimental mouse model dependent on the recently delineated signaling pathway involving EPCR-LBPA.

Conclusions: COVID-19 patients rapidly expand B1a cells secreting pathogenic lipid-binding aPL with broad thrombotic and inflammatory effects. The association with

Anne Hollerbach and Nadine Müller-Calleja equally contributed to this article. Manuscript handled by: Patricia Liaw

This is an open access article under the terms of the Creative Commons Attribution-NonCommercial License, which permits use, distribution and reproduction in any medium, provided the original work is properly cited and is not used for commercial purposes.

© 2021 The Authors. *Journal of Thrombosis and Haemostasis* published by Wiley Periodicals LLC on behalf of International Society on Thrombosis and Haemostasis

NHLBI UM1-HL120877; Deutsche Forschungsgemeinschaft, Grant/Award Number: MU4233/1-1 and SFB1292; Bundesministerium für Bildung und Forschung, Grant/Award Number: 01EO1003 and 01EO1503

markers of inflammation and coagulation, clinical severity, and mortality suggests a causal role of aPL in COVID-19-associated coagulopathy.

KEYWORDS

antiphospholipid antibodies, COVID-19, endothelial protein C receptor, blood coagulation disorder, inflammation

1 | INTRODUCTION

Coronavirus disease 19 (COVID-19)-associated coagulopathy (CAC) has been amply described as a major complication related to disease severity and poor outcome.¹⁻³ Besides venous and arterial thrombotic events, lungs of COVID-19 patients show prominent endothelial injury and widespread thrombosis and capillary microthrombi.⁴ Several potential mechanisms underlying CAC have been proposed^{5,6} including antiphospholipid antibodies (aPL), which have been detected in some COVID-19 patients.⁷⁻⁹ While aPL are causally involved in the pathogenesis of antiphospholipid syndrome (APS), an autoimmune disease characterized by thromboembolic events and pregnancy complications,¹⁰ their functional role in CAC is poorly understood and so far no association with clinical events or death has been described. It should be noted that aPL are also frequently observed transiently during the course of several infectious diseases,¹¹ but these infection-associated aPL have not been considered pathogenic previously.^{10,12}

Catastrophic APS (CAPS) is a rare acute, life-threatening form of APS, characterized by widespread vascular occlusions leading to organ failure. Pulmonary capillaritis, small vessel thrombosis, and diffuse alveolar hemorrhage leading to adult respiratory distress syndrome are major signs of lung involvement in CAPS¹³ and overlap with the pulmonary pathologies observed in severe COVID-19.^{4,6} Importantly, infections are considered a major precipitating factor of CAPS.¹³ Although various aPL reactivities have been observed at different frequency in COVID-19 patients and linked to thrombosis,⁷⁻⁹ no clear mechanisms emerged by which aPL might aggravate the clinical course of infections with the single stranded RNA virus, severe acute respiratory syndrome-coronavirus 2 (SARS-CoV-2).

We have shown that lipid-binding aPL of the IgG isotype are pathogenic *in vivo* and elucidated the underlying signal transduction.¹⁴⁻¹⁷ The cellular target for aPL is the endosomal phospholipid lysobisphosphatidic acid (LBPA) presented by the protein C receptor (EPCR). Binding of the EPCR-LBPA lipid-protein complex by aPL induces a signaling cascade that activates proinflammatory and prothrombotic cellular responses in several cell types including monocytes, dendritic cells, and endothelial cells. Lipid-binding aPL are secreted by CD5⁺CD27⁺CD43⁺ B1a cells in mice. This specific B-cell population rapidly expands *in vitro* and *in vivo* upon stimuli involving the single stranded RNA sensing toll like receptor (TLR)7 and interferon (IFN)- α secreted by dendritic cells. B1a cells with phospholipid reactivity circulate in the blood of mice with experimentally induced autoimmune disease.¹⁴ To gain insights into the role

Essentials

- The pathogenesis of coagulopathy and hyperinflammation in coronavirus disease 19 (COVID-19) is not fully elucidated.
- Antiphospholipid antibodies (aPL) were determined in two cohorts of COVID-19 patients.
- Lipid-binding aPL produced by B1a cells were associated with severity and mortality of COVID-19.
- aPL induce prothrombotic and inflammatory effects by targeting the complex of endothelial protein C receptor and lysobisphosphatidic acid.

of aPL in COVID-19, we analyzed patient sera for the presence of lipid-binding aPL, defined their signaling mechanism, and identified circulating B1 cells as the likely source for these lipid-binding aPL in COVID-19 patients.

2 | METHODS

2.1 | Patients and blood sampling

Two cohorts of 53 and 121 adult patients with PCR-confirmed SARS-CoV-2 infection and COVID-19 were included in our study between March 2020 and February 2021. The severity of COVID-19 was graded as uncomplicated, complicated, or critical according to a classification adapted from the World Health Organization (WHO) classification based on clinical presentation, pulmonary function, and respiratory support (Table S1 in supporting information). Patients with need for invasive ventilation were considered critical, even when an existing health-care directive rejected this therapy. Patients were followed until discharge from the hospital or in-hospital death. Blood samples were drawn at the discretion of the treating physicians as necessary for the clinical management of the patients. Additional laboratory analyses were performed from surplus material as available. Patients were not included if no serum for aPL assays was available. The use of surplus material for research purposes has been approved by the ethics committee of the state medical association of Rheinland-Pfalz, Germany (reference number 2020-14988-2) in accordance with the Declaration of Helsinki.

2.2 | Assays for aPL

aPL were determined in all COVID-19 patients by Quanta Flash automated chemiluminescent immunoassays (Instrumentation Laboratory) for anticardiolipin IgG and IgM, and anti- β 2-glycoprotein I (β 2GPI) IgG and IgM using the cutoffs determined in a large German cohort.¹⁸ Antibodies against the complex of phosphatidylserine and prothrombin (anti-PS/PT) of the IgG and IgM isotype were determined by ELISA (Instrumentation Laboratory) using the cutoff recommended by the supplier (30 CU). Additionally, anticardiolipin and anti-LBPA IgG were determined in a homemade ELISA format that does not contain protein cofactors, as described previously.¹⁹ Briefly, ELISA plates (Nunc Maxisorp™, Thermo Scientific) were coated overnight with 2.5 μ g/well cardiolipin (#C1649, Sigma) or LBPA (#857133P, Avanti Polar Lipids) in 100 μ L ethanol at 4°C. After washing three times in Dulbecco's phosphate buffered saline (DPBS, pH 7.1–7.5, #D8537-500ML, Sigma)/0.1% Tween-20, plates were blocked for 1 h with 1% Tween-20 in DPBS followed by another washing step. 10 μ L serum diluted 1:10 in DPBS were added and incubated 1 h at room temperature (RT). After washing, bound human IgG was detected with horseradish peroxidase-conjugated goat anti-human IgG (#A0293-1ML, Sigma) diluted 1:10,000 (1 h, RT) followed by a final washing step. TMB substrate (#T0440-100ML, Sigma) was incubated 5 min in the dark and the reaction was stopped by adding 2N H₂SO₄. Optical density (OD) was measured at 450 nm (reference 620 nm) using an Ao Microplate Reader (Azure Biosystems, Inc.). The anticardiolipin assay was calibrated using the human monoclonal lipid-binding aPL HL5B and results are reported as arbitrary units (AU). The cutoff for positivity was determined at 26 AU, which represents the mean of 27 randomly picked controls from the local population (participants of the Gutenberg Health Study)¹⁸ plus 3 standard deviations.

2.3 | Isolation of immunoglobulins

Due to the limited availability of serum we used, preferentially, immunoglobulins purified by ammonium sulfate precipitation rather than IgG purified by protein G affinity binding. Immunoglobulins were precipitated in 40% (v/v) saturated ammonium sulfate (#3746.3, Roth) solution for 3 h on ice. The precipitate was collected by centrifugation and the immunoglobulin fraction was resuspended in PBS and desalted using PD MiniTrap G25 columns (#28918007, GE Healthcare) following the manufacturer's instructions. To ascertain that cellular activation was mediated by the IgG-fraction, we isolated IgG from 3 patients with sufficient surplus serum and positive for lipid-binding aPL by protein G affinity adsorption as previously described and determined induction of *TNF* mRNA in monocytes.¹⁴

2.4 | Induction of procoagulant activity

The human monocytic cell line MonoMac 1 (MM1) was exposed to immunoglobulin fractions and procoagulant activity was determined

as previously described.¹⁴ Based on a standard curve of recombinant tissue factor (TF; HemosIL RecombiPlasTin 2G, #0020003051, Instrumentation Laboratory, Munich, Germany) clotting times were converted into procoagulant activity (PCA) units.

2.5 | Cell culture

MM1 cells (#ACC252, DSMZ) were maintained in RPMI-1640 medium (#R0883, Sigma) supplemented with 10% fetal bovine serum (#10270-106, Gibco), L-glutamine (#35050-038, Gibco), nonessential amino acids (#11140-035, Gibco), and sodium pyruvate (#S8636, Sigma) at 37°C with 5% CO₂. Human umbilical vein endothelial cells (HUVEC; #C-12203, Promocell) were grown in complete endothelial cell growth medium (#C-22010, Promocell) at 37°C with 5% CO₂ until confluency in 75 cm² treated cell culture flasks (Corning).²⁰ For stimulation with immunoglobulins, only passages from 2 to 12 were used. Immunoglobulins (10 μ g/mL) were added to MM1 (1 \times 10⁶ cells/mL cultured overnight in 24 well cell culture dishes [Nunclon™ Delta Surface, Thermo Scientific]) or HUVEC (1.25 \times 10⁵ cells/mL seeded overnight in 24-well cell culture dishes [Nunclon™ Delta Surface, Thermo Scientific]). Inhibitors were added 15 min before the stimuli as indicated in Table S2 in supporting information.

2.6 | mRNA expression analysis

For real-time qPCR, total RNA was extracted (RNeasy Mini Kit, #74106, Qiagen) and reverse transcribed (cDNA synthesis kit, #331470L, Biozym). Relative quantification of gene expression was performed by real-time PCR on the CFX Connect Real-Time System (Bio-Rad) using SYBR green (Blue S'Green qPCR Kit, #331416XL, Biozym) normalized to β -actin levels and unstimulated cells. Primer sequences are shown in Table S3 in supporting information.

2.7 | Flow cytometry

aPL-producing B cells were detected in ethylenediaminetetraacetic acid (EDTA) blood by staining with fluorescently labelled phospholipid vesicles as previously described.¹⁴ Fc-receptors were blocked prior to the antibody staining to avoid unspecific labelling of the cells (FcR blocking reagent, #130-059-901, Miltenyi Biotec). Cell surface staining was performed using labeled antibodies listed in Table S4 in supporting information. Soluble EPCR (sEPCR) and sEPCR loaded with LBPA was prepared as described.^{14,21} EDTA blood was stained with phospholipid vesicles or fluorescently labeled β 2GPI and the respective antibodies as indicated for 30 min at 4°C in the dark. After washing with cold PBS/1% BSA cells were incubated with Red blood cell lysis buffer (#420301, BioLegend) for 10 min at RT. Subsequently, cells were pelleted and resuspended in PBS. Fluorescently labeled cells were detected using a FACS Lyric flow cytometer (BD). FlowJo 7.2 software was used for data analysis.

2.8 | Inferior vena cava thrombosis model

aPL-induced thrombus formation *in vivo* was determined as previously described.^{14,17} Immunoglobulins isolated from six critical Covid-19 patients or healthy controls (10 µg) were injected via jugular catheter into wild-type mice 1 h prior to flow reduction in the inferior vena cava (IVC) induced by ligation. Antibodies directed against the endothelial protein C receptor (αEPCR) were injected through the catheter 15 min before immunoglobulins. Rhodamine B-labeled (#R1755, Sigma) platelets and 100 µL of 50 mg/mL Acridine Orange (#A6014, Sigma) to label leukocytes were used to visualize the evolving thrombi. Thrombus formation was imaged by high-speed fluorescence video microscopy using a high-speed wide-field Olympus BX51WI fluorescence microscope.

2.9 | Statistics

Continuous data are shown as means ± standard deviation or median and interquartile range (IQR) as appropriate. To compare two groups GraphPad Prism 8 software was used for unpaired t test or Mann-Whitney test. For multiple comparison one-way analysis of variance (ANOVA) and Tukey's/Dunnett multiple comparison test or Kruskal-Wallis test and Dunn's multiple comparison test or two-way ANOVA and Sidak's multiple comparison test was used. Normal distribution was confirmed using Shapiro-Wilk test. Categorical variables were compared by χ^2 test. A *P*-value of <.05 was considered statistically significant.

3 | RESULTS

We hypothesized that lipid-binding aPL occur during COVID-19 as has been described in other viral diseases. Table 1 summarizes the clinical characteristics of the initial cohort, which consisted of 24 non-critical patients (16 uncomplicated, 8 complicated) and 29 critical patients, based on a WHO criteria-based classification of disease severity (Table S1). As expected, critical patients showed a marked elevation of markers of inflammation (C-reactive protein) and coagulopathy (D-dimer). Concentrations of ferritin and white blood cell counts also tended to be higher in critical patients, but there was a major overlap in the range of measurements between patient groups.

In the commercial clinical routine assays, anticardiolipin IgG titers were significantly higher in critical patients, but the majority of patients in both groups had titers within the reference range. Only a few patients (one non-critical and six critical) had titers above the diagnostic cutoff (Table 1). One critical COVID-19 patient tested positive for anti-β2GPI IgG and none for aPL of the IgM isotype. Four patients (two critical and two non-critical) had antibodies directed against the complex of anti-PS/PT of the IgM isotype. No anti-PS/PT of the IgG isotype were detected (Table 1). Lupus anticoagulant activity, which is caused by autoantibody interference with different

steps in the clotting cascade,²² could not be determined due to insufficient amounts of surplus citrate plasma.

Because commercial assays for anticardiolipin reactivity contain β2GPI and are designed to be less sensitive for lipid-binding aPL,¹² we analyzed the reactivity of patient IgG on ELISA plates coated with cardiolipin alone calibrated with a human monoclonal lipid-binding aPL (HL5B). Critical patients had significantly higher titers than non-critical patients in this assay, which detects lipid-binding aPL of the IgG isotype. They were also more likely to test positive, that is, more than three standard deviations higher titers than the mean of the control group. In the assay format measuring specifically lipid-reactive aPL, 29 of 53 patients were positive (Table 2). Patients with lipid-binding aPL were more often male and had more often a critical course of COVID-19 compared to aPL-negative patients. Patients with aPL had higher concentrations of C-reactive protein, indicating hyper-inflammation, and of D-dimer, reflecting coagulopathy. In the lipid-binding aPL positive group 11 patients died (37.9%) whereas only 3 deaths (12.5%) occurred in the aPL negative group (*P* = .0366; two sided χ^2 -test).

To validate the results observed in the initial cohort we analyzed an additional 121 COVID-19 patients (72 male and 49 female) for lipid-binding aPL. This cohort consisted of 78 non-critical patients (38 uncomplicated, 40 complicated) and 43 critical patients (Tables 3 and 4). The proportion of patients with lipid-binding aPL above the cutoff was 29.5% (23/78) in non-critical patients and 65.1% (28/43) in critical patients (*P* = .0001). Titers of lipid-binding aPL also correlated with clinical severity. In non-critical patients, median titer was 17.4 AU with an IQR of 15.3–27.6 AU. In critical patients, median titer was 37.5 AU with an IQR of 20.9–92.3 AU (*P* < .0001).

We have recently identified LBPA presented by EPCR on the cell surface as an antigenic target for lipid-binding aPL which bind efficiently to cardiolipin and other negatively charged phospholipids in the ELISA format.¹⁴ Therefore, we analyzed serum samples of both cohorts for binding to LBPA in an ELISA. Correlation between anticardiolipin and anti-LBPA results expressed as optical density was very good (r^2 = 0.8654; Figure S1 in supporting information). These data suggested EPCR-LBPA as the target for aPL developing in COVID-19 patients.

Lipid-binding aPL in mice are secreted by a circulating population of B1a cells. This population expands dependent on TLR7 signaling and secretion of IFN-α by dendritic cells.¹⁴ We therefore analyzed peripheral blood B cells in 10 patients of the cohort described above. We identified a distinct circulating B cell population reactive with fluorescently labeled phospholipid vesicles; these B cells were not detectable in healthy controls and represented approximately 25% of circulating CD19⁺ lymphocytes (Figure 1A,B). Notably, COVID-19 patients had no B cells that were reactive with β2GPI or prothrombin (Figure 1B), while B cells reactive with β2GPI can be readily detected in patients with APS (Figure S2 in supporting information). This is in line with the low prevalence of aPL directed against β2GPI in the present study and other series of COVID-19 patients.⁷⁻⁹ Phospholipid-reactive B cells expressed CD20, CD27, and CD43 and were IgG positive (Figure 1D,E), but lacked CD38 expression. This

TABLE 1 Characteristics of the first cohort of COVID-19 patients. Data are shown as median (interquartile range)

	Non-critical patients (n = 24)	Critical patients (n = 29)	P-value
Age (mean ± SD)	63.9 ± 15.3	64.8 ± 17.1	n.s.
Sex (m/f)	11/13	19/10	n.s.
Fatal outcome (n)	0	14	<.0001
Body mass index (kg/m ²)	27.8 (24.3–33.6)	26.9 (25.4–32.5)	n.s.
Preexisting disease			
Arterial hypertension	15	12	n.s.
Cardiovascular disease	9	5	n.s.
Diabetes mellitus	4	5	n.s.
Respiratory diseases	2	6	n.s.
Anticoagulation			
None	2	1	n.s.
Prophylactic	19	5	<.0001
Therapeutic	3	23	<.0001
Dexamethasone	6	15	.0477
Remdesivir	0	5	.0326
CRP (mg/L)	27 (16–63)	174 (110–213)	<.0001
Ferritin (µg/L)	417 (222–1,172)	968 (352–2,813)	n.s. (.0569)
D-dimer (mg/L FEU)	0.8 (0.5–1.3)	2.2 (1.4–4.0)	.0001
WBC (1/nl)	5.6 (4.2–8.3)	9.0 (7.3–9.8)	.0120
Lymphocytes (1/nl)	0.9 (0.7–1.5)	0.9 (0.5–1.4)	n.s.
Platelets (1/nl)	192 (123–238)	201 (150–327)	n.s.
Lipid binding aPL (AU)	20.2 (16.6–23.6)	45.7 (30.7–79.3)	<.0001
Pos./neg.	5/19	24/5	<.0001
Anticardiolipin IgG (CU)	2.8 (2.6–4.6)	5.8 (4.3–13.9)	.0026
Pos./neg.	1/23	6/23	n.s. (.0770)
Anticardiolipin IgM (CU)	1.9 (1.0–3.2)	2.1 (1.0–3.3)	n.s.
Pos./neg.	0/24	0/29	n.s.
Anti-β2GPI IgG (CU)	6.0 (6.0–6.9)	10.1 (6.0–15.1)	.0019
Pos./neg.	0/24	1/28	n.s.
Anti-β2GPI IgM (CU)	1.0 (1.0–1.3)	1.1 (1.1–1.1)	.0371
Pos./neg.	0/24	0/29	n.s.
Anti-PS/PT IgG (CU)	4.0 (3.3–5.1)	4.4 (3.7–6.2)	n.s.
Pos./neg.	0/24	0/29	n.s.
Anti-PS/PT IgM (CU)	3.4 (1.1–10.3)	7.3 (2.8–18.9)	n.s.
Pos./neg.	2/22	2/29	n.s.

T-test or two-sided Mann-Whitney U-test for continuous data; two sided χ^2 -test for categorical data.

Abbreviations: COVID-19, coronavirus disease 19; CRP, C-reactive protein; n.s., not significant; PS/PT, phosphatidylserine and prothrombin; SD, standard deviation; WBC, white blood cell.

profile is typical for B1a cells, although this subtype is not as well defined by surface markers in humans as it is in mice.²³ Recent studies have demonstrated an expansion of plasmablasts in COVID-19 patients during acute infection, which is likely related to the SARS-CoV-2-specific antibody response.²⁴ This response is apparently very rapid, because it can build on existing germline sequences in the population that require few somatic mutations to gain specificity for SARS-CoV-2.²⁵ Plasmablasts related to this response express

CD38 but not CD20, demonstrating that they are distinctly different from the phospholipid-binding B cell population described here.

Lipid-reactive aPL only bind to sEPCR after exchange of the structurally bound phosphatidylcholine with LBPA.¹⁴ We therefore studied the ability of recombinant sEPCR to compete binding of labeled phospholipid vesicles to B cells. Only sEPCR loaded with LBPA (sEPCR-LBPA), but not unmodified sEPCR effectively competed binding of phospholipid vesicles to B cells circulating in COVID-19

	aPL-negative patients (n = 24)	aPL-positive patients (n = 29)	P-value
Age (mean ± SD)	63.8 ± 15.7	64.8 ± 16.9	n.s.
Sex (m/f)	11/13	18/11	n.s.
Clinical severity			
Uncomplicated	14 (58.33%)	2 (6.90%)	<.0001
Complicated	5 (20.83%)	3 (10.34%)	n.s.
Critical	5 (20.83%)	24 (82.76%)	<.0001
Fatal outcome	3 (12.5%)	11 (37.9%)	.0366
CRP (mg/L)	50.5 (16.8–124.0)	127 (69–205)	.0110
Ferritin (µg/L)	407 (233–955)	1288 (330–2,784)	n.s. (.0784)
D-dimer (mg/L FEU)	0.8 (0.5–1.2)	2.1 (1.4–4.0)	<.0001
WBC (1/nl)	6.4 (3.9–8.6)	9.0 (6.3–11.1)	.0172
Lymphocytes (1/nl)	0.9 (0.6–1.5)	0.9 (0.7–1.4)	n.s.
Platelets (1/nl)	175 (119–232)	234 (150–332)	n.s.

TABLE 2 Comparison of aPL-positive and aPL-negative patients

Note: T-test or two-sided Mann-Whitney U-test for continuous data; two sided χ^2 -test for categorical data.

Abbreviations: aPL, antiphospholipid antibodies; CRP, C-reactive protein; n.s., not significant; SD, standard deviation; WBC, white blood cell.

TABLE 3 Characteristics of the second cohort of COVID-19 patients. Data are shown as median (interquartile range)

A	Missing data	Non-critical patients (n = 78)	Critical patients (n = 43)	P-value
Age (mean ± SD)	0	69.5 ± 16.0	68.2 ± 11.7	n.s.
Sex (m/f)	0	40/38	32/11	.0131
Fatal outcome (n)	0	4	25	<.0001
CRP (mg/L)	0	65 (32–111)	153 (118–253)	<.0001
Ferritin (µg/L)	45 (27/18)	504 (167–1207)	1328 (643–2470)	.0003
D-dimer (mg/L FEU)	20 (17/3)	1.1 (0.8–2.0)	1.7 (0.9–3.3)	n.s. (.0501)
WBC (1/nl)	0	5.9 (4.4–8.0)	9.0 (5.7–13.3)	.0029
Lymphocytes (1/nl)	9 (8/1)	0.9 (0.6–1.3)	0.8 (0.4–1.2)	.0301
Platelets (1/nl)	0	204 (165–273)	194 (146–270)	n.s.
Lipid binding aPL (AU)	0	17.4 (15.3–27.6)	37.5 (20.9–92.3)	<.0001
Pos./neg.		23/55	28/15	.0001
Anticardiolipin IgG (CU)	1 (1/0)	3.3 (2.6–5.9)	3.1 (2.6–6.3)	n.s.
Pos./neg.		4/74	0/43	n.s.
Anticardiolipin IgM (CU)	1 (1/0)	2.5 (1.2–4.3)	2.3 (1.4–3.4)	n.s.
Pos./neg.		0/78	0/43	n.s.
Anti-β2GPI IgG (CU)	1 (1/0)	6.0 (6.0–6.0)	6.0 (6.0–7.1)	n.s.
Pos./neg.		1/77	0/43	n.s.
Anti-β2GPI IgM (CU)	1 (1/0)	(1.0–2.0)	1.0 (1.0–2.0)	n.s.
Pos./neg.		1/77	1/42	n.s.

T-test or two-sided Mann-Whitney U-test for continuous data; two sided χ^2 -test for categorical data.

Abbreviations: aPL, antiphospholipid antibodies; COVID-19, coronavirus disease 19; CRP, C-reactive protein; n.s., not significant; SD, standard deviation; WBC, white blood cell.

patients (Figure 1C). Taken together, these data demonstrated the expression of an IgG B cell receptor reactive with EPCR-LBPA, which represents the pathogenic target previously implicated in autoimmune pathology of APS.¹⁴

Lipid-binding aPL induce inflammatory and procoagulant genes (*TNF*, *F3* [tissue factor]) by activating a pathway dependent on complement crosstalk with TF-dependent signaling and downstream activation of endosomal nicotinamide adenine

TABLE 4 Comparison of aPL-positive and aPL-negative patients

	Missing data	aPL-negative patients (n = 70)	aPL-positive patients (n = 51)	P-value
Age (mean ± SD)	0	67.5 ± 15.4	71.2 ± 13.2	n.s.
Sex (m/f)	0	36/34	36/15	.0340
Clinical severity				
Uncomplicated	0	30 (42.86%)	8 (15.69%)	.0015
Complicated		25 (35.71%)	15 (29.41%)	n.s.
Critical		15 (21.43%)	28 (54.90%)	.0001
Fatal outcome	0	11 (15.7%)	18 (35.3%)	.0127
CRP (mg/L)	0	61 (28–120)	139 (98–220)	<.0001
Ferritin (µg/L)	45 (24/21)	580 (204–1433)	996 (488–1588)	n.s.
D-dimer (mg/L FEU)	20 (15/5)	1.1 (0.6–1.5)	2.4 (1.3–5.9)	<.0001
WBC (1/nl)	0	5.9 (4.4–8.8)	7.7 (5.1–11.7)	.0331
Lymphocytes (1/nl)	9 (7/2)	0.9 (0.5–1.4)	0.8 (0.6–1.1)	n.s.
Platelets (1/nl)	0	197 (154–259)	228 (168–275)	n.s.

Note:: T-test or two-sided Mann-Whitney U-test for continuous data; two sided χ^2 -test for categorical data.

Abbreviations: CRP, C-reactive protein; n.s., not significant; SD, standard deviation; WBC, white blood cell.

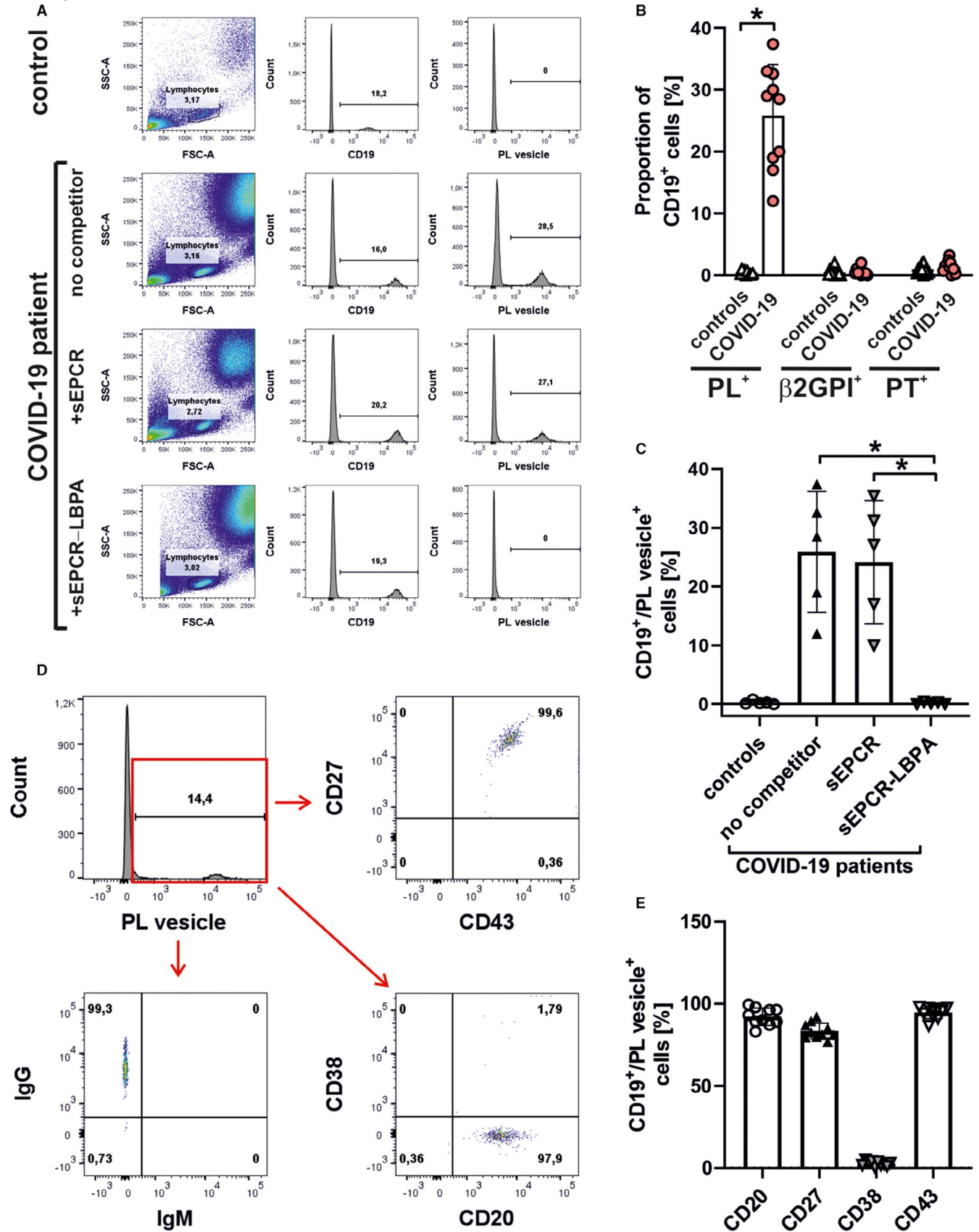
dinucleotide phosphate (NADPH) oxidase, which is a critical intermediate of aPL signaling.^{15,16} These aPL responses and the induction of interferon-regulated genes, for example, *IRF8* and *GPB6*, are dependent on specific binding of aPL to cell surface EPCR, which is lipid exchanged to LBPA by endolysosomal recycling.¹⁴ Immunoglobulin isolated from 10 COVID-19 patients similarly induced the expression of *TNF*, *F3*, *IFR8*, and *GPB6* in the monocytic cell line MM1 (Figure 2A). All effects were prevented by the complement factor 3 inhibitor compstatin and inhibitory (α EPCR 1496), but not non-inhibitory (α EPCR 1489) monoclonal antibodies against human EPCR, as we have previously shown for lipid-binding aPL from APS patients.¹⁴ In three patients we obtained sufficient amounts of serum to purify IgG by protein G adsorption. Purified IgG from these patients also induced *TNF* in monocytes, providing additional evidence that the relevant lipid-binding aPL are of the IgG isotype (Figure S3 in supporting information).

In addition, aPL induce a rapid decryption of cell surface TF on monocytes and complement-dependent thrombosis.²⁶ COVID-19 patient immunoglobulins also rapidly decrypted cell surface TF and this activation was blocked by anti-EPCR or sEPCR loaded with LBPA, but not the unmodified sEPCR carrying the typical structurally bound phosphatidylcholine (Figure 2B). This and prior studies indicated that most COVID-19 patients do not develop aPL directed against β 2GPI.^{7–9} Unlike lipid-reactive aPL, which induce a rapid but transient induction of *TNF* *in vitro*, β 2GPI-specific aPL induce *TNF* only after prolonged stimulation for 12–15 h.²⁷ *TNF* induction by COVID-19 aPL was no longer observed in monocytes after 12 h, while β 2GPI-reactive IgG from APS patients significantly induced *TNF* at this time point (Figure 2C). These data further indicated that

no functionally relevant anti- β 2GPI reactivity was present in these patient sera.

Since activation of the endothelium has been described in COVID-19 pathology, we extended our *in vitro* analysis to this cell type. Immunoglobulin from COVID-19 patients also rapidly induced *TNF* and *F3* in HUVEC (Figure 2D). As observed in monocytic cells, this activation was also dependent on complement, EPCR, and endosomal reactive oxygen species (ROS), the latter shown by prevention of endosomal ROS generation by the inhibitor of endosomal superoxide generation niflumic acid (NFA; Figure 2E). It should be noted that an immunocompromised patient with COVID-19 neither developed anti-SARS-CoV-2 antibodies nor aPL. Immunoglobulin isolated from this patient did not elicit the signaling effects observed in aPL-positive patients. Thus, COVID-19 polyclonal immunoglobulin induces the previously delineated aPL autoimmune signaling pathway by targeting the EPCR--LBPA complex presented on the cell surface.

Human monoclonal lipid-binding aPL and polyclonal aPL isolated from autoimmune mice accelerate thrombus formation *in vivo* dependent on complement and EPCR--LBPA.^{14,16,17} A recent publication linked the prothrombotic activity of COVID-19 aPL to reactivity with phosphatidylserine/prothrombin and primarily prothrombin itself, although the study also found other aPL specificities.⁸ Patients in our cohort with lipid-reactive aPL rapidly induced TF and EPCR-dependent signaling. We therefore evaluated *in vivo* whether this mechanism or alternative pathways may contribute to thrombosis upon injection of immunoglobulin from six critical COVID-19 patients (median anticardiolipin titer 78.8 AU, range 72.1–244 AU). Compared to immunoglobulin isolated from healthy controls, COVID-19 immunoglobulin significantly accelerated thrombus formation in an established flow-restricted IVC thrombosis model for APS (Figure 3).



Thrombus growth was comparable to previously observed effects of lipid-binding aPL.^{14,16,17} We applied a specific inhibitory antibody to EPCR-LBPA (αEPCR 1682) and a binding, but non-inhibitory

control antibody (αEPCR 1650) to define the underlying mechanism of COVID-19 immunoglobulin-induced thrombosis.¹⁴ Note that both antibodies to EPCR have no effect on EPCR-dependent protein

FIGURE 1 Flow cytometric analysis of circulating B cells in coronavirus disease 19 (COVID-19) patients. A, Representative example of flow cytometric detection of peripheral blood B cells reactive with fluorescently labeled phospholipid (PL) vesicles. Left panels represent the whole blood scatter plot, middle panels show the proportion of CD19 positive lymphocytes, and right panels show the proportion of CD19 positive lymphocytes reactive with PL vesicles. Recombinant soluble endothelial protein C receptor (sEPCR) with structurally bound phosphatidylcholine or lipid-exchanged sEPCR-- lysobisphosphatidic acid (LBPA) were included as competitor during the PL staining. B, Staining of CD19-positive B cells with labeled PL vesicles, β 2GPI, or prothrombin (PT) in 10 healthy controls and 10 COVID-19 patients. * $P < .0001$, two-way analysis of variance (ANOVA), Sidak's multiple comparisons test. C, Competition of sEPCR or sEPCR-LBPA with PL vesicle staining of CD19-positive B cells in 5 COVID-19 patients. * $P < .001$; one-way ANOVA, Dunnett multiple comparison test. D, Characterization of surface marker expression by PL vesicle-reactive B cells in COVID-19 patients. Representative scatter plots demonstrating CD27, CD43, CD20, and IgG expression in the absence of CD38 and IgM staining. E, Quantification of B cell surface marker expression in 10 COVID-19 patients

C activation. The protective effect of anti-EPCR 1682 (Figure 3) demonstrated that COVID-19 immunoglobulin accelerated thrombus formation by the same EPCR--LBPA--dependent signaling pathway as we described previously for lipid-binding aPL in autoimmune pathologies.¹⁴

4 | DISCUSSION

We present evidence in two cohorts of patients hospitalized for COVID-19 that approximately 45% of all patients developed lipid-binding aPL of the IgG isotype above the cutoff determined in healthy controls. The appearance of these lipid-reactive aPL is much higher than the prevalence of β 2GPI-dependent anticardiolipin antibodies, anti- β 2GPI, or anti-PS/PT detected in our patients with commercially available assays and described by others in COVID-19.⁷⁻⁹ Lipid-reactive aPLs are known to rapidly appear in acute and chronic infections and have been specifically linked to viral diseases.¹¹ While infection-associated aPL have previously been considered non-pathogenic, there is no conclusive evidence to support this view. For example, in viral hepatitis B and C and cytomegalovirus (CMV) infections aPL are commonly detected. For hepatitis C, the presence of anticardiolipin is associated with an approximately 3-fold increased incidence of thrombotic complications.²⁸ Similarly, CMV infection increases the risk for thrombosis about 3-fold and acute coronary syndrome 2.5-fold. However, an association with aPL titers has not been established.²⁹ In this study, we observed a significant association of the presence and titers of lipid-binding aPL with severity of COVID-19 and mortality from SARS-CoV-2 infection. This suggests a specific role of lipid-binding aPL in the development of lethal COVID-19 disease.

A limitation of our study is the single-center, retrospective, observational design, which did not permit inclusion of all COVID-19 patients. In particular, younger patients with mild to moderate disease were discharged early without availability of serum for aPL determination. This is reflected in the high proportion of critical patients in the first cohort. We therefore analyzed a second cohort with a focus on available aPL results for disease severity and mortality.

We have previously shown in mice that lipid-binding aPL significantly accelerate thrombus formation by activation of a complex signaling pathway involving EPCR--LBPA, TF, acid sphingomyelinase, and complement. Mice with genetic defects in this pathway

are protected from the pathogenic effects of lipid-binding aPL. Similarly, targeting key components of the pathway with specific antibodies or drugs prevents thrombus formation in autoimmune disease.^{14,16,30} We show that immunoglobulin fractions from COVID-19 patients who tested positive for lipid-binding aPL--IgG bind to the autoimmune target EPCR--LBPA on the cell surface and elicit the same responses *in vitro* and *in vivo* as pathogenic lipid-binding aPL observed in APS and autoimmune disease. Due to the small amount of serum available we had to use ammonium sulfate precipitation to obtain immunoglobulins rather than the specific purification of IgG by protein G adsorption. However, in three patients we could confirm that cellular effects were mediated by protein G-purified IgG. Furthermore, we unequivocally show that the immunoglobulin fractions specifically activate *in vitro* and *in vivo* the signaling pathway delineated for lipid-binding aPL of the IgG isotype.¹⁴ In particular, we show here that a specific antibody blocking the signaling of EPCR--LBPA completely abrogated accelerated thrombus formation following injection of COVID-19 immunoglobulin in our mouse model. This indicates that the pathogenic effects of COVID-19 immunoglobulin can be ameliorated with strategies that are effective in autoimmune disorders and APS-associated thrombosis.

Lipid-binding aPL in mice are produced by a specific B1a cell population.¹⁴ In COVID-19 patients we identified a B-cell population reactive with EPCR--LBPA and the typical features of B1a cells. In mice, aPL sustain prolonged TLR7-dependent activation of B1a cells reactive with EPCR--LBPA.¹⁴ Analogous to autoimmune disease, activation of endosomal, RNA-sensing TLRs following infection with SARS-CoV-2 may lead to an initial activation of preexisting B1a cells producing lipid-reactive aPL and subsequent expansion of these B1a-cells supported by innate immune cell activation mediated by aPL triggering EPCR--LBPA and endosomal TLR7 signaling (Figure 4).

The pathological features of microcirculatory collapse documented in COVID-19 include leukocyte activation, platelet deposition, and micro-thrombotic vessel occlusion.^{31,32} Here we add rapid decryption of the coagulation initiator TF and induction of its expression by COVID-19 aPL as a probable cause for excessive coagulation. The central role for TF in pathogenesis has already been demonstrated in other severe viral infections.³³ Levels of circulating TF-bearing extracellular vesicles are correlated with D-dimer levels and increased specifically in patients with severe COVID-19.^{34,35} Genetic susceptibility to severe COVID-19 has furthermore been linked to TF as well as coagulation and complement regulatory proteins.³⁶ Together with the robust activation of inflammatory and

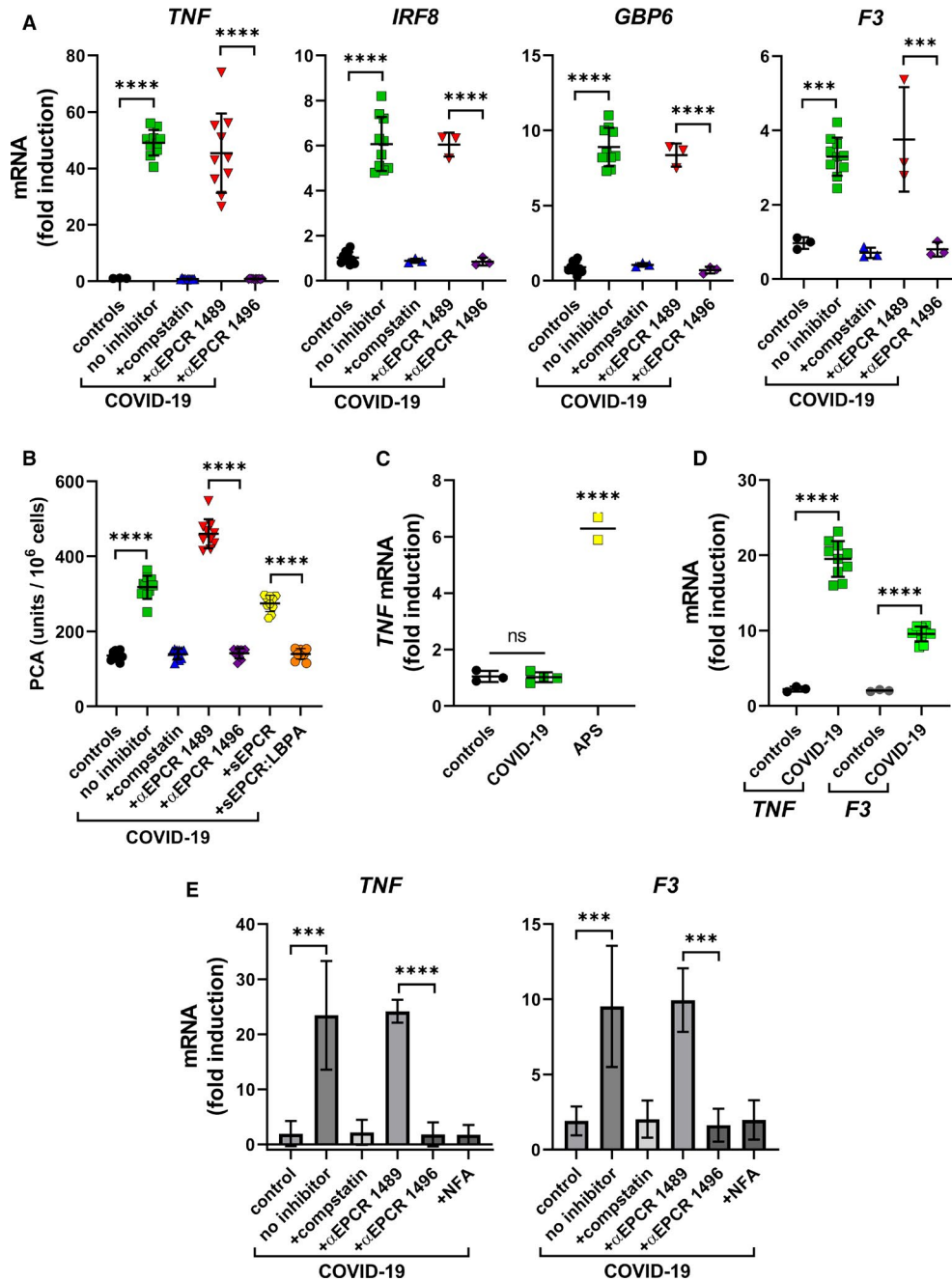


FIGURE 2 COVID-19 immunoglobulins induce proinflammatory and procoagulant genes in monocytes and endothelial cells. **A**, Induction of mRNA expression in MonoMac 1 (MM1) cells by immunoglobulin (10 μ g/ml) isolated from COVID-19 patients or healthy controls. MM1 were stimulated for 3 h (*TNF*) or 1 h (*IRF8*, *GBP6*, *F3*) with or without the complement inhibitor compstatin (2 μ g/ml), inhibitory (α EPCR 1496) or non-inhibitory (α EPCR 1489) (mean \pm standard deviation (SD), $n \geq 3$). **** $P < .0001$, *** $P = .0002$; one-way analysis of variance (ANOVA) and Tukey's multiple comparisons test. **B**, Procoagulant activity (PCA) after stimulation of monocytic MM1 cells by immunoglobulin (10 μ g/ml) was measured by single-stage clotting assay in triplicates; mean \pm SD, $n = 10$. **** $P < .0001$; one-way ANOVA and Tukey's multiple comparisons test. **C**, Delayed induction of *TNF* mRNA in monocytic MM1 cells by stimulation with immunoglobulins (10 μ g/ml) for 12 h; mean \pm SD, $n \geq 2$; **** $P < .0001$; one-way ANOVA and Tukey's multiple comparisons test. **D**, *TNF* and *F3* mRNA expression in human umbilical vein endothelial cells (HUVEC) stimulated for 3 h with immunoglobulins (10 μ g/ml); mRNA expression was normalized to the positive control lipopolysaccharide (LPS); mean \pm SD, $n = 3$, **** $P < .0001$; one-way ANOVA and Tukey's multiple comparisons test. **E**, Inhibition of immunoglobulin induction (10 μ g/ml isolated from one representative COVID-19 patient) of *TNF* and *F3* mRNA in HUVEC by compstatin (2 μ g/ml), inhibitory (α EPCR 1496) or non-inhibitory (α EPCR 1489), or the endosomal reactive oxygen species (ROS) inhibitor niflumic acid (NFA) (10 μ g/ml); mRNA expression was normalized to the positive control LPS; mean \pm SD, $n \geq 3$; **** $P < .0001$, *** $P \leq .001$. T-test or Mann-Whitney test following Shapiro-Wilk test for normal distribution

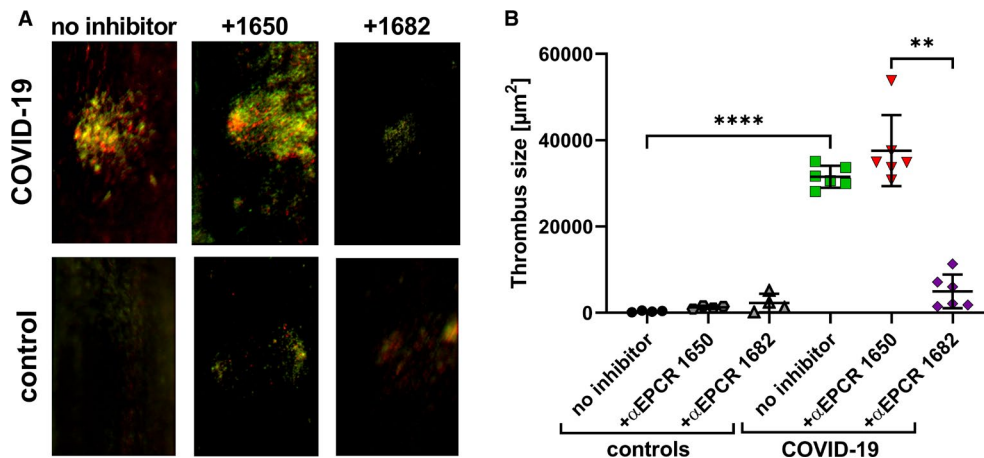


FIGURE 3 Coronavirus disease 19 (COVID-19) immunoglobulin promotes thrombus formation by signaling via endothelial protein C receptor (EPCR). A, Representative images of thrombus formation in mice treated with immunoglobulin (10 μg) isolated from a healthy control or a COVID-19 patient. Platelets are shown in red and leukocytes are shown in green. B, Quantification of thrombus size in vena cava inferior 3 h after injection of immunoglobulin isolated from healthy controls (n = 4) or COVID-19 patients (n = 6) and flow restriction in the inferior vena cava. To demonstrate involvement of EPCR, mice were treated with inhibitory (αEPCR 1682) or non-inhibitory (αEPCR 1650) antibodies 15 min before injection of immunoglobulin. Mean ± standard deviation, n = 4. ****P < .0001, **P = .0022, t-test or Mann-Whitney test following Shapiro-Wilk test for normal distribution

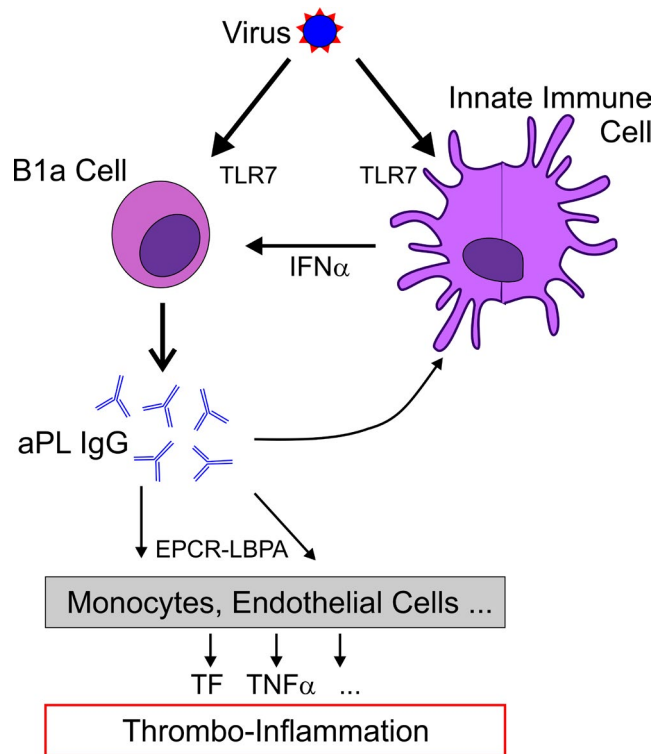


FIGURE 4 Schematic overview of the proposed pathway of viral RNA-induced expansion of pathogenic antiphospholipid antibodies (aPL) in coronavirus disease 19 (COVID-19). Contact with virus leads to intensive activation of innate immune cells (e.g., plasmacytoid dendritic cells) with participation of TLR7 and secretion of IFNα, which induces aPL production by B1a cells.¹⁴ This initiates a positive feedback loop with dendritic cells and induces procoagulant and inflammatory responses for example in monocytes and endothelial cells.

complement pathways,³⁷ clinical and laboratory aspects of severe COVID-19 resemble observations in CAPS.¹³ Mutations in complement regulatory genes have recently been implicated in the pathogenesis of (C)APS³⁸ and coagulation-complement crosstalk is also critical in the signal transduction of lipid-binding aPL.

TF upregulation in immune and vascular cells is a common event elicited by viral infection. Induction of TF-initiated coagulation in this context may thus be amplified by the acute expansion of aPL-producing B1a cells leading to the severe micro-thrombotic acute respiratory distress syndrome in severely ill COVID-19 patients. In addition to thrombosis, the TF pathway directly participates in innate immune signaling and immune evasion.³⁹⁻⁴¹ Because titers of lipid-binding aPL were correlated not only with coagulation activation, but also the extent of inflammation, clinical severity, and fatal outcome, effective anticoagulant strategies in COVID-19 may require targeting TF for added anti-inflammatory benefit and improved patient outcome.

The delayed onset of severe manifestations of COVID-19 is consistent with a two-stage model of initial virus-induced host response followed by prothrombotic and proinflammatory exacerbation driven by signaling of lipid-binding aPL. Moreover, the capacity of aPL to perpetuate an autoimmune signaling loop by targeting EPCR-LBPA should be taken into consideration as a possible cause for the slow recovery in certain patients with long COVID syndrome. Thus, our data implicate lipid-reactive aPL in the development of the thrombo-inflammatory syndrome associated with a more severe clinical course of COVID-19.

ACKNOWLEDGMENTS

This study was funded by the National Institutes of Health (NHLBI UM1-HL120877), the Humboldt Foundation of Germany (Humboldt

Professorship Ruf), the Federal Ministry of Education and Research Germany (BMBF 01EO1003 and 01EO1503), the German Center for Cardiovascular Research (DZHK), and the German Research Foundation (MU4233/1-1, SFB1292). The funders had no role in the study design or collection and interpretation of data.

CONFLICTS OF INTEREST

W. Ruf, K.J. Lackner, N.Müller-Calleja, and L. Teyton are inventors on a patent “Methods for detection of pathogenic antiphospholipid antibodies and for identification of inhibitors” (PCT/EP2020/085278) and provisional patent applications for COVID-19 therapy. W.R. is a consultant for ARCA biopharma. All other authors (A.H., D.P., A.C., M.F.S., T.F., H.R., M.B., C.W., I.S., T.M., O.S., V.S., M.R., J.N., P.R.G.) have no conflict of interest to report.

AUTHOR CONTRIBUTIONS

A. Hollerbach and N.Müller-Calleja collected data, performed experiments, and wrote the manuscript; D. Pedrosa performed the *in vivo* mouse experiments; A. Canisius performed experiments; T. Falter and H. Rossmann collected laboratory data; M.F. Sprinzl, M. Bodenstern, C. Werner, I. Sagoschen, T. Münzel, O. Schreiner, V. Sivanathan, M. Reuter, J. Niermann, and P.R. Galle were responsible for patient care and collected clinical data; L. Teyton provided critical reagents; W. Ruf and K.J. Lackner conceived and designed the study, and wrote and edited the manuscript.

ORCID

Anne Hollerbach  <https://orcid.org/0000-0002-3831-2152>

Martin F. Sprinzl  <https://orcid.org/0000-0002-4544-9560>

Heidi Rossmann  <https://orcid.org/0000-0002-7532-8540>

Wolfram Ruf  <https://orcid.org/0000-0002-6064-2166>

Karl J. Lackner  <https://orcid.org/0000-0002-1985-7931>

REFERENCES

- Zhou F, Yu T, Du R, et al. Clinical course and risk factors for mortality of adult inpatients with COVID-19 in Wuhan, China: a retrospective cohort study. *Lancet*. 2020;395:1054-1062.
- Guan WJ, Ni ZY, Hu Y, et al. Clinical characteristics of coronavirus disease 2019 in China. *N Engl J Med*. 2020;382:1708-1720.
- Tang N, Li D, Wang X, Sun Z. Abnormal coagulation parameters are associated with poor prognosis in patients with novel coronavirus pneumonia. *J Thromb Haemost*. 2020;18:844-847.
- Ackermann M, Verleden SE, Kuehnel M, et al. Pulmonary vascular endothelialitis, thrombosis, and angiogenesis in Covid-19. *N Engl J Med*. 2020;383:120-128.
- Merrill JT, Erkan D, Winakur J, James JA. Emerging evidence of a COVID-19 thrombotic syndrome has treatment implications. *Nat Rev Rheumatol*. 2020;16:581-589.
- Iba T, Warkentin TE, Thachil J, Levi M, Levy JH. Proposal of the definition for COVID-19-associated coagulopathy. *J Clin Med*. 2021;10:191.
- Devreese KMJ, Linskens EA, Benoit D, Peperstraete H. Antiphospholipid antibodies in patients with COVID-19: a relevant observation? *J Thromb Haemost*. 2020;18:2191-2201.
- Zuo Y, Estes SK, Ali RA, et al. Prothrombotic autoantibodies in serum from patients hospitalized with COVID-19. *Sci Transl Med*. 2020;12:eabd3876.
- Taha M, Samavati L. Antiphospholipid antibodies in COVID-19: a meta-analysis and systematic review. *RMD Open*. 2021;7:e001580.
- Schreiber K, Sciascia S, de Groot PG, et al. Antiphospholipid syndrome. *Nat Rev Dis Primers*. 2018;4:17103.
- Sène D, Piette J-C, Cacoub P. Antiphospholipid antibodies, antiphospholipid syndrome and infections. *Autoimmun Rev*. 2008;7:272-277.
- Devreese KMJ, Ortel TL, Pengo V, de Laat B, Subcommittee on Lupus Anticoagulant/ Antiphospholipid Antibodies. Laboratory criteria for antiphospholipid syndrome: communication from the SSC of the ISTH. *J Thromb Haemost*. 2018;16:809-813.
- Rodríguez-Pintó I, Moitinho M, Santacreu I, et al. CAPS Registry Project Group (European Forum on Antiphospholipid Antibodies). Catastrophic antiphospholipid syndrome (CAPS): descriptive analysis of 500 patients from the international CAPS registry. *Autoimmun Rev*. 2016;15:1120-1124.
- Müller-Calleja N, Hollerbach A, Royce J, et al. Lipid presentation by the protein C receptor links coagulation with autoimmunity. *Science*. 2021;371:eabc0956.
- Prinz N, Clemens N, Strand D, et al. Antiphospholipid-antibodies induce translocation of TLR7 and TLR8 to the endosome in human monocytes and plasmacytoid dendritic cells. *Blood*. 2011;118:2322-2332.
- Müller-Calleja N, Hollerbach A, Ritter S, et al. Tissue factor pathway inhibitor primes monocytes for antiphospholipid antibody-induced thrombosis. *Blood*. 2019;134:1119-1131.
- Manukyan D, Müller-Calleja N, Jäckel S, et al. Cofactor independent human antiphospholipid antibodies induce venous thrombosis in mice. *J Thromb Haemost*. 2016;14:1011-1020.
- Manukyan D, Rossmann H, Schulz A, et al. Distribution of antiphospholipid antibodies in a large population-based German cohort. *Clin Chem Lab Med*. 2016;54:1663-1670.
- Müller-Calleja N, Köhler A, Siebald B, et al. Cofactor-independent antiphospholipid antibodies activate the NLRP3-inflammasome via endosomal NADPH-oxidase: implications for the antiphospholipid syndrome. *Thromb Haemost*. 2015;113:1071-1083.
- Prinz N, Clemens N, Canisius A, Lackner KJ. Endosomal NADPH-oxidase is critical for induction of the tissue factor gene in monocytes and endothelial cells. Lessons from the antiphospholipid syndrome. *Thromb Haemost*. 2013;109:525-531.
- Disse J, Petersen HH, Larsen KS, et al. The endothelial protein C receptor supports tissue factor ternary coagulation initiation complex signaling through protease-activated receptors. *J Biol Chem*. 2011;286:5756-5767.
- Noordermeer T, Molhoek JE, Schutgens REG, et al. Anti-β2-glycoprotein I and anti-prothrombin antibodies cause lupus anticoagulant through different mechanisms of action. *J Thromb Haemost*. 2021;19:1018-1028.
- Quách TD, Rodríguez-Zhurbenko N, Hopkins TJ, et al. Distinctions among circulating antibody-secreting cell populations, including B-1 cells, in human adult peripheral blood. *J Immunol*. 2016;196:1060-1069.
- Bernardes JP, Mishra N, Tran F, et al. Longitudinal multi-omics analyses identify responses of megakaryocytes, erythroid cells, and plasmablasts as hallmarks of severe COVID-19. *Immunity*. 2020;53:1296-1314.
- Kreer C, Zehner M, Weber T, et al. Longitudinal isolation of potent near-germline SARS-CoV-2-neutralizing antibodies from COVID-19 patients. *Cell*. 2020;182:1663-1673.
- Müller-Calleja N, Ritter S, Hollerbach A, Falter T, Lackner KJ, Ruf W. Complement C5 but not C3 is expendable for tissue factor activation by cofactor-independent antiphospholipid antibodies. *Blood Adv*. 2018;2:979-986.
- Müller-Calleja N, Hollerbach A, Häuser F, Canisius A, Orning C, Lackner KJ. Antiphospholipid antibody induced cellular responses depend on epitope specificity – implications for treatment of APS. *J Thromb Haemost*. 2017;15:2367-2376.

28. Ambrosino P, Lupoli R, Tarantino P, Di Minno A, Tarantino L, Di Minno MN. Viral hepatitis and anti-phospholipid antibodies positivity: a systematic review and meta-analysis. *Dig Liver Dis.* 2015;47:478-487.
29. Kelkar AH, Loc BL, Tarantino MD, et al. Cytomegalovirus-associated venous and arterial thrombotic disease. *Cureus.* 2020;12:e12161.
30. Müller-Calleja N, Manukyan D, Canisius A, Strand D, Lackner KJ. Hydroxychloroquine inhibits proinflammatory signalling pathways by targeting endosomal NADPH oxidase. *Ann Rheum Dis.* 2017;76:891-897.
31. Nicolai L, Leunig A, Brambs S, et al. Immunothrombotic dysregulation in COVID-19 pneumonia is associated with respiratory failure and coagulopathy. *Circulation.* 2020;142:1176-1189.
32. Skendros P, Mitsios A, Chrysanthopoulou A, et al. Complement and tissue factor-enriched neutrophil extracellular traps are key drivers in COVID-19 immunothrombosis. *J Clin Invest.* 2020;130:6151-6157.
33. Geisbert TW, Hensley LE, Jahrling PB, et al. Treatment of Ebola virus infection with a recombinant inhibitor of factor VIIa/tissue factor: a study in rhesus monkeys. *Lancet.* 2003;362:1953-1958.
34. Rosell A, Havervall S, von Meijenfeldt F, et al. Patients with COVID-19 have elevated levels of circulating extracellular vesicle tissue factor activity that is associated with severity and mortality. *Arterioscler Thromb Vasc Biol.* 2021;41:878-882.
35. Guervilly C, Bonifay A, Burtsey S, et al. Dissemination of extreme levels of extracellular vesicles: tissue factor activity in patients with severe COVID-19. *Blood Adv.* 2021;5:628-634.
36. Ramlall V, Thangaraj PM, Meydan C, et al. Immune complement and coagulation dysfunction in adverse outcomes of SARS-CoV-2 infection. *Nat Med.* 2020;26:1609-1615.
37. Yan B, Freiwald T, Chauss D, et al. SARS-CoV-2 drives JAK1/2-dependent local complement hyperactivation. *Sci Immunol.* 2021;6:eabg0833.
38. Chaturvedi S, Braunstein EM, Yuan X, et al. Complement activity and complement regulatory gene mutations are associated with thrombosis in APS and CAPS. *Blood.* 2020;135:239-251.
39. Zelaya H, Rothmeier AS, Ruf W. Tissue factor at the crossroad of coagulation and cell signaling. *J Thromb Haemost.* 2018;16:1941-1952.
40. Antoniak S, Mackman N. Multiple roles of the coagulation protease cascade during virus infection. *Blood.* 2014;123:2605-2613.
41. Graf C, Wilgenbus P, Pagel S, et al. Myeloid cell-synthesized coagulation factor X dampens antitumor immunity. *Sci Immunol.* 2019;4:eaaw8405.

SUPPORTING INFORMATION

Additional supporting information may be found online in the Supporting Information section.

How to cite this article: Hollerbach A, Müller-Calleja N, Pedrosa D, et al. Pathogenic lipid-binding antiphospholipid antibodies are associated with severity of COVID-19. *J Thromb Haemost.* 2021;19:2335-2347. <https://doi.org/10.1111/jth.15455>